Graphical Abstract

Surface-Subsurface flow effect on earthen dikes geomechanical stability during overtopping event

Nathan Delpierre, Hadrien Rattez, Sandra Soares-Frazão

Highlights

Surface-Subsurface flow effect on earthen dikes geomechanical stability during overtopping event

Nathan Delpierre, Hadrien Rattez, Sandra Soares-Frazão

- A coupled surface-subsurface flow model has been developed.
- Evolution of the water content shows a big influence on the longitudinal and lateral slope stability during an overtopping event.
- The model reproduces well the water content evolution and slope instability of small scale experimental data.

Surface-Subsurface flow effect on earthen dikes geomechanical stability during overtopping event

Nathan Delpierre[a], Hadrien Rattez[a], Sandra Soares-Frazão[a]

[a] *Institute of Mechanics Materials and Civil Engineering, UCLouvain, Louvain-la-Neuve, Belgium*

Abstract

Droughts and extreme precipitation events, exacerbated by climate change, are causing growing threats to earthen dams. The increasing frequency of extreme events, which were not always considered when these earthen structures were built means that these factors may not have been fully accounted for in their design. The risk of overtopping flow is therefore increased and the initial soil's saturation level has a significant impact on the structure's strength that should not be overlooked during the assessment of the dike risk of failure when overtopped. In this paper, we present an innovative physically-based numerical framework to investigate how combined surface-subsurface flows affect slope stability.

In this paper, we present a novel numerical framework that consists in a physically-based approach which allows to study the effects of combined surface-subsurface flows on the slope stability evolution, using an effective stress formulation for the mechanical analysis. The surface flows are described using a one-dimensional shallow-water equations solver and are coupled in a conservative way with the subsurface flow, through a two-dimensional Richards equation solver. The shear strength reduction method is employed, in combination with an effective stress approach, to assess the longitudinal and lateral slope safety factor evolution taking into account the pore-pressure and saturation degree changes in time during overtopping.

Keywords: surface-subsurface flow, Dike overtopping, Unsaturated soil mechanics, Slope stability, Shear strength reduction method

Preprint submitted to Geomechanics for Energy and the Environment *October 8, 2024*

1. Introduction

Geotechnical structures made of soil, such as dams and dikes, play a crucial role in managing floods, facilitating fluvial transport, and disposing of mining wastes. The consequences of their failure can be severe, resulting in human casualties, destruction of cities, and damage to infrastructure.

In September 2023, the city of Derna in Libya experienced the devastating aftermath of two consecutive dam failures. The Mansour dam, located 12 km upstream of Derna and designed to hold 22.5 million cubic meters of water, collapsed after an overtopping event likely due to intense rainfall from the storm Daniel. The massive volume of water cascaded towards the Derna dam, located near the city, triggering a second dam failure. This chain of events resulted in an estimated 20,000 human casualties and widespread devastation in the city. These two consecutive dam failures are representative of many issues related to dam and dikes exploitation in the current global warming context.

In particular, two phenomena can be pointed out when dealing with such structures in the current global warming context. First, the increasing frequency of long droughts and extreme precipitation events leads earthen structures to undergo high variations of internal water content. When long droughts occur, dessication cracks might appear due to high suction pressures[1]. This phenomenon locally leads to mechanically weaker zones but also to fast infiltration paths for water, during subsequent rainfall events. On the other hand, long wet periods can lead to a decrease of shear strength in the soil when it becomes saturated or close to saturation, which can result in the dam's failure. Second, the return periods for extreme precipitation events, considered for the design of these structures, are currently showing a significant decrease[2]. This suggests that many structures designed in the past for events with a (e.g) 100-year return period may now be undersized for the more intense events of the 21st century.

Failure of earthen dams are complex phenomena. In 34% of the cases, they are triggered by overtopping events[3]. It combines fast erosive flows that generate a deep channel with geomechanical block failure on the breach sides. Tingsanchali et al.[4] investigated the competition between the longitudinal slope failure and the erosive process using a numerical model and small scale experiments for sandy dikes. Their findings highlighted that the influence of longitudinal slope failure was important to consider in downstream slopes with a height-length ratio below 1:2.5, emphasizing that the erosive process alone was insufficient to fully characterize the underlying physical phenomena. As most river dikes have a downstream slope ratio of 1:2, the longitudinal sliding should thus be considered to model accurately their failure.

The dynamics of breach opening play a major role in the way water rushes into areas that should be protected by dams or dikes. This is why numerical models have been developed with the aim of making better predictions of breach outflows. Nevertheless, most of these models are based on the idea that the breaching is mostly dominated by the erosion process of a non-cohesive material. Therefore, these models consist in solving the shallow-water equations combined with the Exner equation, which is a mass conservation equation[5],[6],[7]. To perform a reliable simulation, specific sediment transport laws are required to catch the general behaviour of the system. The choice of the appropriate law is in general critical for the simulation quality and require specific calibration, as underlined by Van Emelen et al.[8]. Tingsanchali et al.[4] used such a model combined with a slope stability model based on limit equilibrium, but they did not solve for the water infiltration and their results show a critical role of an empirical parameter that estimates the pore water pressure inside the dam.

It should be noted that, especially for cohesive materials, the flow through the breach is also influenced to a large extent by the breach widening resulting from lateral block failures[9], while the erosive process mainly participates to the breach deepening. Some attempts to consider these lateral blocks failures led to the developments of simplified numerical models, such as the bank failure operator, developed by Swartenbroekx et al.[10], which consists in adjusting the slopes based only on a given friction angle. Recent works by Zhong et al.[11] or Xue et al.[12] proposed to account for lateral block failures by using the limit equilibrium method. While a sediment transport law is used for the breach deepening, a planar block collapse is supposed for the breach sides.

These simplified method do not account for soil saturation that also significantly affects the mechanical strength of the dam, which evolves greatly when the dam is exposed to intense rainfalls, droughts and overtopping. Such evolutions are clearly identified as landslides triggering effects and cannot be disregarded[13]. In recent years, extensive research has been conducted to investigate the mechanical behaviour of unsaturated soils, building upon the foundational contributions of Bishop[14]. The exploration of the role of suction and soil saturation on shear strength gave rise to a substantial research effort, leading to the development of new constitutive models using two stress state variables, such as the Barcelona Basic Model[15], or models based on the effective stress principle[16]. Arguments against the validity of the effective stress in unsaturated soils argue that it cannot explain the volumetric collapse phenomenon upon wetting[17], but as here we are interested only in the shear failure, both approaches lead to similar results. Moreover, effective stress approach provides a smooth transition from unsaturated to saturated states, which is particularly useful for cases involving fluctuations of the water table like for dikes and dams. Effective stress approaches also requires less model parameters than total stress approaches and capture well the evolution of the shear strength with suction[16].

In this paper, we present an innovative numerical modelling framework for the dynamic assessment of the safety factor of earthen embankments during overtopping. By integrating a coupled surface-subsurface flow solver from Delpierre et al.[18] with an effective stress approach from Alonso et al.[16], our model provides a robust and physically based method. Using only measurable quantities such as the soil-water retention curve and shear strength, the model is able to provide valuable insight into the potential failure of a given embankment during an overtopping event.

The present paper is divided in 3 different sections. In section 2, we recall our methodology to solve in a coupled way the surface and subsurface flows. Section 3 describes the constitutive model we use to describe the influence of suction pressure on the shear strength of the soil. Finally, in section 4, we combine the outcomes of the coupled surface-subsurface flows solver with the effective stress approach. This results in a comprehensive model, able to predict the evolution of the dike's stability under various theoretical situations.

We successfully compare our model with experimental data from the literature, accurately predicting the failure onset of an experimental dike subjected to a specific overtopping event. This alignment with experimental results provides additional confidence in our methodology.

2. Coupled surface-subsurface flows

2.1. Subsurface flow: the Richards equation

Based on a combination of the Darcy law and mass conservation principle, the Richards equation describes water transfers in porous unsaturated and saturated media, such as soils. In a mixed form, meaning the simultaneous presence of suction and water content terms, the Richards equation can be written as follows:

$$\frac{\partial \theta(h)}{\partial t} - \nabla[K(h)\nabla(h+z)] = 0 \tag{1}$$

where θ is the volumetric water content, h the pore pressure and K the hydraulic conductivity. The high non-linearity associated to the Richards equation mainly results from the constitutive law employed to describe the relationship between pore pressure and the other physical parameters, θ and K. In this work, we make use of the classical Mualem-van Genuchten constitutive law, describing the so-called soil-water retention curve (SWRC; see Fig.(1)). These relationships, describing the transitioning effects between saturated and unsaturated soils, are explicitly provided in Delpierre et al.[18].

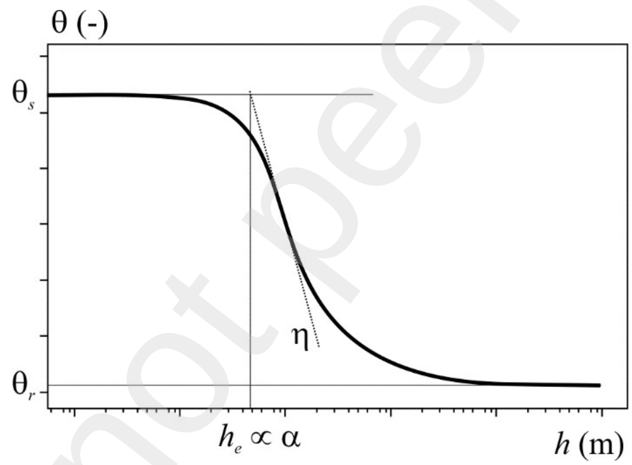

Figure 1: Example soil-water retention curve (following[18]).

Fig. 1 recalls the main parameters leading any SWRC shape. θ_s is the saturated volumetric water content, θ_r the residual water content. These values constitute the bounds for the water content of a given soil. These quantities are also used to express the equivalent volumetric water content as

$$S_e = \frac{\theta - \theta_r}{\theta_s - \theta_r}. \tag{2}$$

The parameter α is, together with the saturated hydraulic conductivity K_s, the one which influence in the most critical way the saturation process. It is inversely proportionally linked to the air-entry pressure, usually defined as the pressure required for the water to escape from a saturated soil. Typically, in sand-like soil, we can expect low air-entry pressure for this parameter and quite high air-entry pressure values for clay-like soil.

The numerical resolution scheme and its validation have been extensively described in Delpierre et al.[18]. The solver is based on a finite volume formulation with an implicit temporal integration. The terms are obtained by applying the Gauss-Ostrogradsky's theorem to Eq. (1). As the process of groundwater flow can be considered as slow, the implicit formulation conveniently allows big time steps. At each time step, a system of equation is solved and the state variables (θ, h, K) are updated in each cell of the mesh.

2.2. Surface flow and system coupling

As presented in Delpierre et al.[18], we use the shallow-water equations to evaluate the surface flow. Based on mass and momentum conservation principle, this system describes how waters level and velocities evolve in time. Considering a unit-width system, the equations can be written as follows:

$$\frac{\partial h}{\partial t} + \frac{\partial q}{\partial x} = q_{\mathrm{in}} \tag{3}$$

$$\frac{\partial q}{\partial t} + \frac{\partial}{\partial x}\left(\frac{q^2}{h} + g\frac{h^2}{2}\right) = gh\left(S_0 - S_f\right) \tag{4}$$

where h stands for water depth, q the unit discharge, S_0 the bed slope and S_f the friction slope with friction losses evaluated through the Manning's friction formulation. A finite volume scheme with an explicit time integration combined with fluxes evaluated using Roe's scheme is employed as presented in Soares-Frazao and Zech[19].

Spatially, both physical domains are fully coupled. The one-dimensionnal shallow-water equations cells are aligned with the two-dimensionnal triangular cells depicting the geometry of the subsurface domain. With this feature, no error propagation through reinterpolation of physical quantities are expected. In a temporal perspective, the model is decoupled. We take advantage of the implicit nature of the Richards equation solver and of the relatively slow subsurface flow velocity to use large time steps. As regards the surface flow, the explicit nature of the solver implies the use of small time steps according to the CFL condition. The Richards equation solver time step is thus a multiple of the surface flow time step to allow for exchange of information between the two flow domains.

Strict mass conservation is achieved using a proper definition for the source term q_{in}, as described in Delpierre et al.[18], which depicts exchanges between the surface and subsurface flow.

3. Effective stress constitutive model for unsaturated soil

3.1. On the effective stress principle

The effective stress principle is defined by Khalili et al.[20] as the macroscopic effect on the soil skeleton, which means that the effective stress should be seen as the stress responsible for strain. In the context of unsaturated soil, Bishop[14] initially formulated effective stresses as follows:

$$\sigma'_{ij} = \sigma_{ij} + \chi s \delta_{ij} \tag{5}$$

where σ'_{ij} represents the effective stress tensor, σ_{ij} is the total stress tensor, $s = \gamma_w h$ denotes the suction pressure and χ stands for the effective stress parameter. Combining equation(5) with the Mohr Coulomb criterion, gives the following theoretical expression for the shear strength:

$$\tau = c' + \sigma \tan(\phi) + \chi s \tan(\phi) \tag{6}$$

where c' stands for the cohesion and ϕ is the friction angle. It is noteworthy that χ should be equal to one in a saturated soil and zero for a completely dry soil[20]. While the χ parameter has often been considered equivalent to the saturation degree S_e, it was initially intended to be more general. Nevertheless, this definition, while satisfactory for coarse granular soils, falls short in explaining the behavior of finer-grained soils like clay[16]. The main concern with using the saturation degree S_e as representation of χ for clay soil arises from the unrealistic shear strength reached during a drying process, as the product $S_r s$ tends to extremely large values. As highlighted by Alonso et al.[16], it is commonly observed that as the saturation degree decreases, the impact of pore pressure on shear strength diminishes. Following this observation, Alonso et al.[16] proposed a formulation that considers two distinct contributions for the saturation degree:

$$S_e = S_r^m + S_r^M \tag{7}$$

where S_r^M is the macroscopic degree of saturation, describing the presence of water in the macropores, which can evolve in time. S_r^m stands for the microscopic degree of saturation, describing the water content in the micropores. This quantity does not change in time and is independent from load and applied suction. This particular feature allows to differentiate between granular soil and fine soil with higher clay content. In a granular soil, we can expect that water can escape from the pores during a drying process leading to $S_r^m = 0$. On the contrary, as the clay content increases, the microscopic degree of saturation S_r^m should increase accordingly as water can be trapped in small pores.

Following all these developments, Alonso et al.[16] defined an effective degree of saturation such that:

$$S_{\mathrm{r}}^{\mathrm{e}} = \chi = \left\langle \frac{S_{\mathrm{e}} - S_{\mathrm{r}}^{\mathrm{m}}}{1 - S_{\mathrm{r}}^{\mathrm{m}}} \right\rangle \tag{8}$$

with $\langle x \rangle = 0.5(x + |x|)$ corresponding to the Macauley brackets. According to this formulation, χ becomes an expression describing the available water in the macropores, ranging from 0, when water only remains in micropores, to 1, for a fully saturated soil.

3.2. Numerical validation

To validate the implementation of the effective stress formulation, we conducted a comparison between direct shear test data sourced from the literature and finite element method numerical simulations performed using the Moose software[21].

The comparison is based on the direct shear tests conducted by Vanapalli et al.[22] on glacial till. The soil, characterized by a specific sand/silt/clay distribution of respectively 28%, 42%, and 30%, underwent a drying process over several days. The measured friction angle was $\phi = 25°$, and an effective cohesion of zero was observed. Multiple tests were carried out with matric suction ranging from 0 to 500 kPa, maintaining a constant normal confining stress of 25 kPa. The experiments were performed using a modified direct shear test apparatus designed by Gan et al.[23]. Alonso et al.[16] proposed to fit the soil-water retention curve using a pore-air entry pressure related parameter $\alpha = 7.2e^{-05} cm^{-1}$, $\eta = 0.59$, $\mu = 0.67$ and a microscopic degree of saturation $S_{\mathrm{r}}^{\mathrm{m}} = 0.64$.

The direct shear test are conducted numerically using a unit cubic cell. The prescribed boundary conditions included a normal confining pressure of 25 kPa and a continuously increasing horizontal displacement applied to the top, while the bottom of the cell remained fully fixed.

As depicted in Fig.(2), the numerical results exhibit a strong correlation with the experimental shear strength data. The commonly assumed relationship, where χ is considered equal to the saturation degree, is also illustrated (labelled as Bishop shear strength). It can be observed that this assumption proves to be unrealistic for the considered glacial till soil, as the shear strength does not constantly increase over time.

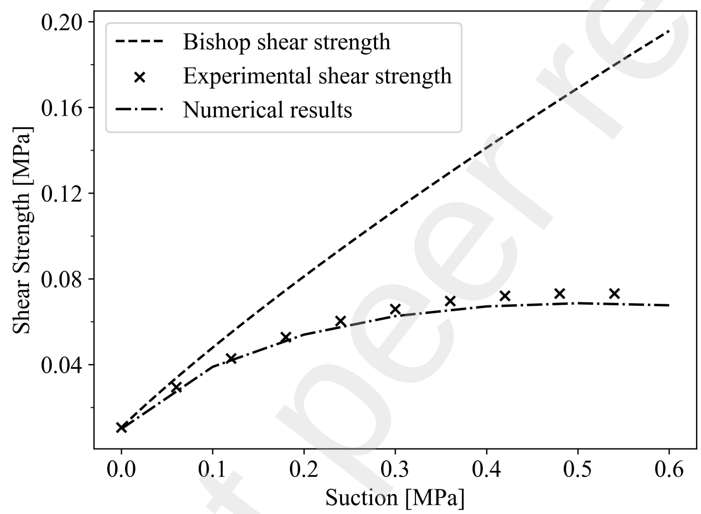

Figure 2: Comparison of numerical and exprimental direct shear test results.

The numerical validation shows that integrating the concept of microscopic degree of saturation enhances the accuracy of shear strength evolution predictions. This aspect will be further explored in the subsequent section, which is dedicated to practical applications.

4. Model application

In this section, we combine the subsurface-surface flow model with the effective stress model to study realistic cases. The safety factor is assessed at various time intervals during a dam overtopping event, employing the shear-strength reduction method (SSRM). This method, first described by Matsui et al.[24], consists in reducing in a linear way the geomechanical properties in the Mohr-Coulomb criteria (see Eq.(6)), defined by a cohesion and a friction angle, until convergence is no longer achieved in the FEM calculation:

$$c'_{SF} = \frac{c'}{SF}, \quad \phi_{SF} = \frac{\phi}{SF} \tag{9}$$

where c'_{SF} is the reduced cohesion and ϕ_{SF} is the reduced friction angle. The resulting reduction factor corresponds to the so-called safety factor (SF). Contrariwise to Limit Equilibrium Methods (LEM), the failure surface does not need to be guessed. In addition, suction, which provides additional strength to the soil, is easily taken into account by remapping the solution of the groundwater flow to Gauss points constituting the FEM mesh.

Aplications of this method are presented in the next sections. First a sensitivity analysis is conducted to investigate the influence of initial conditions and soil-water retention curve parameters. The longitudinal sliding failure mechanism is studied in subsection 4.1 whereas subsection 4.2 is dedicated to transversal side failure. Then, subsection 4.3 shows a successful validation of the model through a comparison with an experimental example retrieved from the literature.

4.1. Longitudinal sliding failure

To enhance comprehension across various cases, the same dam geometry, described in Fig.(3), is used for both longitudinal failure test cases. It consists in an asymetric dam with a 1:3 upstream slope and a 1:2 downstream slope with a 3 m crest height. The initial conditions for the geomechanical calculation consist in a the pore pressure distribution within the dam, obtained by solving the subsurface flow. The influence of both fully saturated and unsaturated regions, as well as their temporal changes, in relation to the stability of the dam is highlighted in subsection 4.1.1.

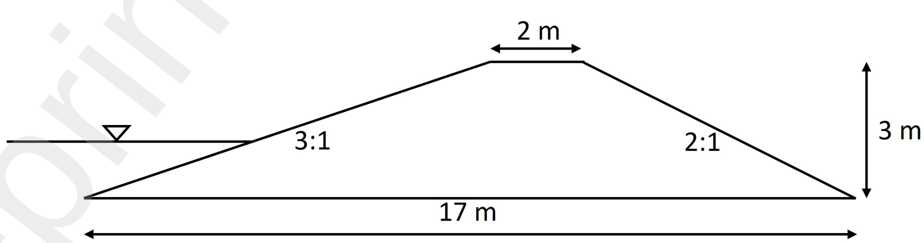

Figure 3: Asymetric dike geometry.

The soil hydraulic properties employed in both section 4.1.1 and section 4.1.2 are identical and are described in Table 1, with the exception of the pore air-entry pressure α, whose influence is specifically investigated in section 4.1.2. A cohesion $c' = 5$ kPa and a friction angle $\phi = 25°$ are considered for the geomechanical properties.

Parameter	Value	Unit	Parameter	Value	Units
K_s	0.001	cm s^{-1}	α	$7.2e^{-05}$	cm^{-1}
θ_r	0.05	-	$\hat{\eta}$	0.59	-
θ_s	0.6	-	μ	0.67	-

Table 1: Soil-water retention curve properties.

During the overtopping event, generated by a constant upstream flow of 200 $l.s^{-1}$, we expect the failure mechanism to develop at the downstream part of the dam as no load is available to counterbalance the internal pore pressure.

4.1.1. Influence of the initial saturation degree

Throughout a classical exploitation, an earthen dam undergoes various meteorological conditions. Rain and droughts significantly affect the soil's water content and thus its shear strength. In this test case, we compare the evolution of the safety factor during an overtopping event for an initially dry dike, corresponding to a homogeneous initial pore pressure $h = -400cm$, and for an initially wet dike, with an initial pore pressure $h = -40cm$. Fig.(4) shows the pore pressure distribution after a 300 s flow for both initial conditions. The steady state is already reached for the wet dike, whereas the water struggles to infiltrate the dry dike.

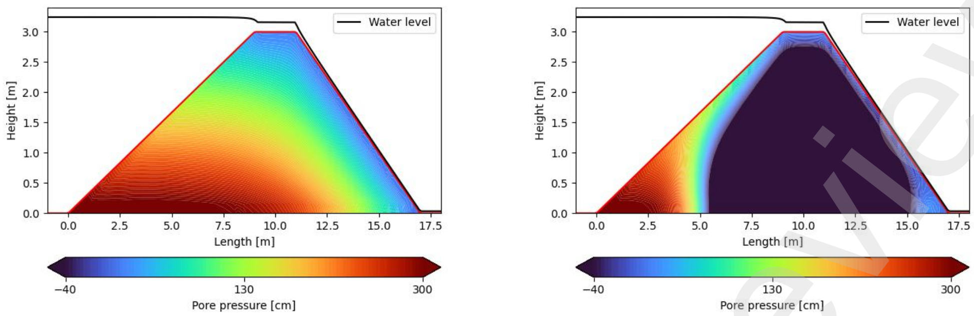

(a) Pore pressure distribution for the wet dike. (b) Pore pressure distribution for the dry dike.

Figure 4: Comparison of the pore pressure distribution after 300 s.

As observed in Fig.(5), the safety factor is influenced to a large extent by the initial water content condition. The decrease in safety factor, associated with the evolution of the saturation degree in the dam during the overtopping, is particularly pronounced in the case of the initially wet dam. Notably, the time to reach the threshold safety factor of 1.5 is observed to be four times faster for the initially wet dam than for the initially dry one.

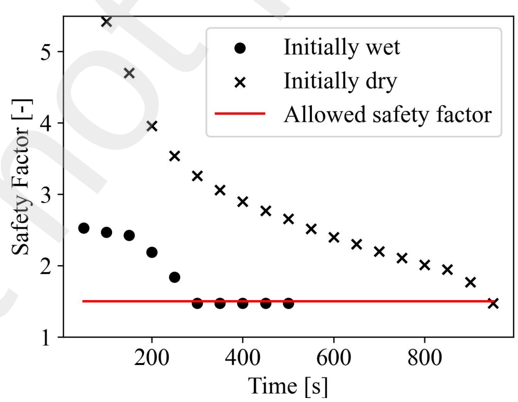

Figure 5: Safety Factor comparison for different initial conditions.

The initial presence of water influences greatly the infiltration rate as water tends to circulate in the already filled areas. These results allow to underline the need of maintaining proper saturation degree conditions inside a dam in operation.

4.1.2. Influence of pore air entry pressure

Among the parameters of the soil-water retention curve, the pore air-entry pressure seems to be the one which influences the most the shear strength. By strongly influencing the value of the α parameter, it also strongly influences the saturated water content plateau (see Fig.(1)). If the α parameter is low, the soil tends to stay at high volumetric water content values even for high suction pressures. This particular behavior causes the soil to reach full saturation more rapidly, consequently accelerating the reduction in mechanical capacities. This, in turn, results in a faster decline of the safety factor, as illustrated in Fig.(6).

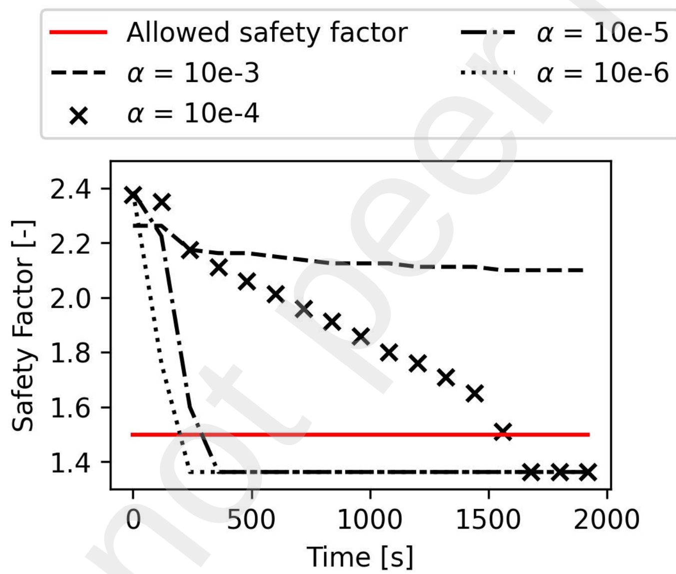

Figure 6: Safety Factor comparison for different pore-air entry pressure.

4.2. Breach widening

In this test case, the lateral breach widening is studied. The influence of the initial groundwater level, which is a result of the past hydrological conditions, on the potential breach side failure is emphasized. The geometry of the test case is presented in Fig.(7), where the water table is represented as well as a water depth representing the flow in the normal direction.

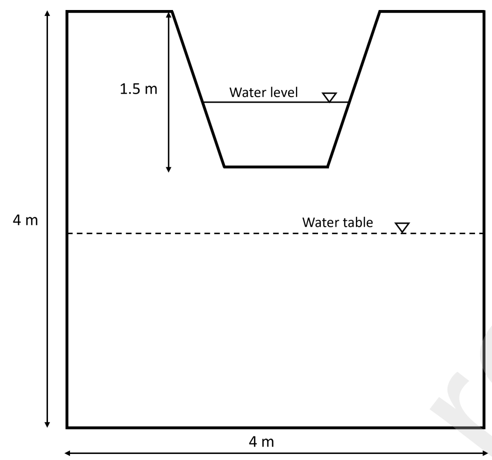

Figure 7: Geometry of the test case.

A 50 cm water depth is considered in the breach and the soil's hydraulic parameters are presented at Table 2.

Parameter	Value	Unit	Parameter	Value	Units
K_s	0.01	cm s^{-1}	α	10^{-3}	cm^{-1}
θ_r	0.05	-	$\hat{\eta}$	2	-
θ_s	0.6	-	μ	0.5	-

Table 2: Soil-water retention curve properties.

The same soil's geomechanical properties are used than in the previous section: a 5 kPa cohesion and a 25° friction angle with a microscopic degree of saturation $S_r^m = 0.8$.

The pore pressure evolves in time and a specific distribution is obtained depending on the initial groundwater level as observed in Fig.(8).

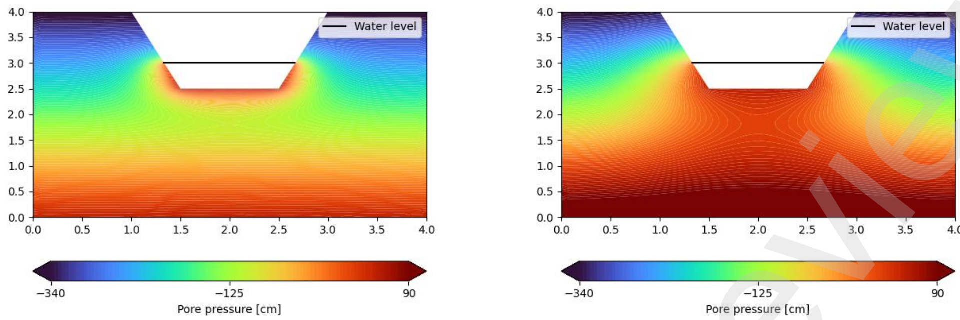

(a) Pore pressure distribution at t = 10 s. (b) Pore pressure distribution at t = 50 s.

Figure 8: Pore pressure evolution for a 0.5 m high initial groundwater level.

The safety factor is evaluated for each scenario after a 50-second groundwater flow simulation, providing an objective basis for comparing the different cases. A rotational block failure mechanism is visible as the FEM calculation stops to converge. An illustration of a typical potential failure surface can be seen at Fig.(9). This shows that in the case of a cohesive material, led by suction forces, a rotational failure mechanism is likely observed rather than a slide failure.

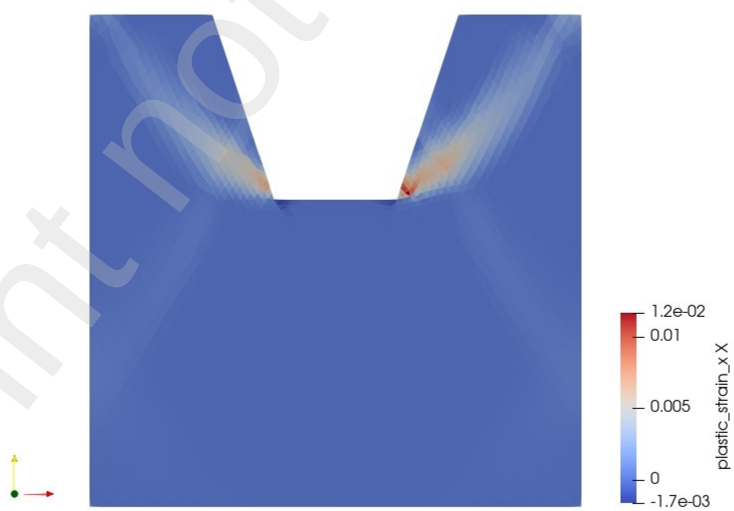

Figure 9: Rotational failure surface.

The safety factor associated to each situation is strongly influenced by the initial groundwater level, as shown at Fig.(10). This is mainly due to the fact that the initial groundwater level influences the rate of saturation in the dam. The higher the initial groundwater level, the lower the safety factor becomes. Again, this underlines the importance of maintaining an optimal degree of saturation in earthen structures. It can be concluded that keeping optimal saturation degrees is crucial in the way breaching will propagate laterally due to block failures.

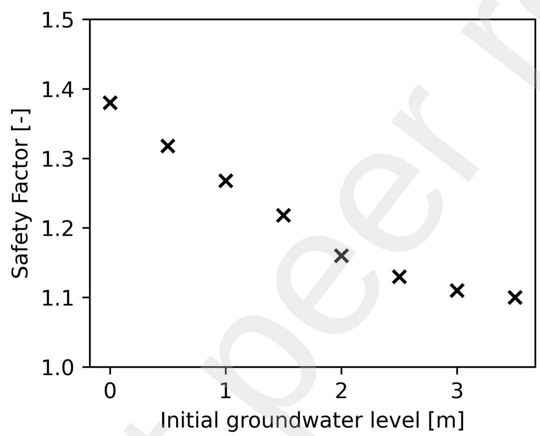

Figure 10: Safety Factor comparison for different initial groundwater level after 50s.

4.3. An experimental test case: dam overtopping

Awal et al.[25] presented the results of various experimental overtopping embankment failures. One of these tests exhibited a geomechanical failure by longitudinal sliding caused by the combined action of surface flow forces and the variation in water content in the soil. The geometry of the test case is represented in Fig.(11).

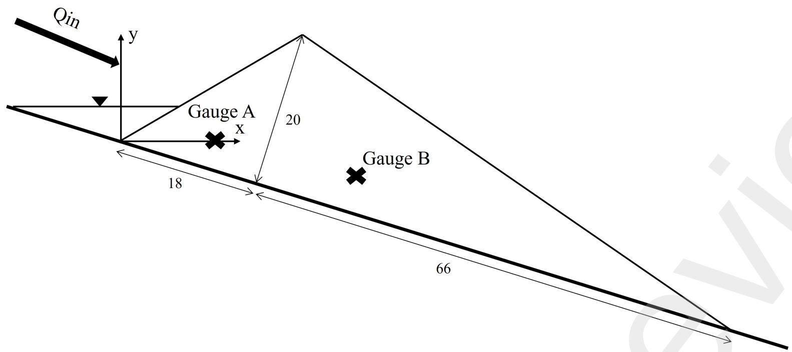

Figure 11: Geometry of the test case.

It consists of a sandy dike, built on a 5-meter long slope, with a steep upstream slope and a smoother downstream slope. The soil-water retention curve parameters were measured and are described in Table 3. Initially the saturation degree S_e is set to 20 %.

Parameter	Value	Unit	Parameter	Value	Units
K_s	0.03	cm s^{-1}	α	0.055	cm^{-1}
θ_r	0.045	-	$\hat{\eta}$	3.2	-
θ_s	0.287	-	μ	0.312	-

Table 3: Soil-water retention curve properties.

The geomechanical properties of the sand are the one of a cohesionless sand with a 34° friction angle.

A 30.5 $cm^3 s^{-1}$ constant inflow discharge was imposed at the upstream end of the setup. The sandy dike is overtopped after approximatively 300 s and a sliding failure is observed after 447 s.

4.3.1. Comparison with the coupled surface-subsurface flows model

The outcomes generated by the numerical model were compared with the volumetric water content data recorded at two gauges throughout the experiment. Although the exact positions of these gauges were not explicitly specified in the original paper, they were estimated to be at the coordinates listed in Table 4.

Initial simulations with the parameters of Table 3 resulted in an overshoot in the saturation degree evolution, with the model response outpacing

Gauge	X	Y
A	0.13	0
B	0.31	-0.05

Table 4: Gauges position.

the measured data. Given the significant uncertainties associated with both gauge positions and the measurement of saturated hydraulic conductivity, the latter parameter was adjusted to $K_s = 0.015\ cm.s^{-1}$, which remains in the same order of magnitude. The final results are presented at Fig.(12), where the wetting process is compared and visually validated.

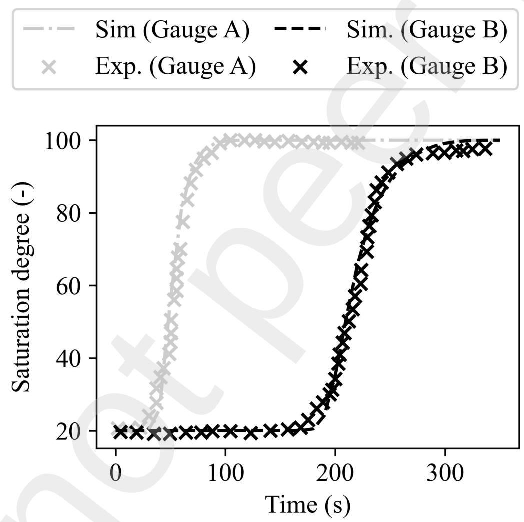

Figure 12: Comparison between experimental (crosses) and numerical results (dashed).

4.3.2. Safety factor evolution

The safety factor is assessed during the event using the shear strength reduction method detailed earlier. Considering the nature of the soil, with likely coarse grains, a microscopic degree of saturation $S_r^m = 0$ was selected. Also, a 60 Pa cohesion was considered for the material, preventing local non physical convergence of the SSRM process. The safety factor evolved greatly throughout the event as shown on Fig.(13).

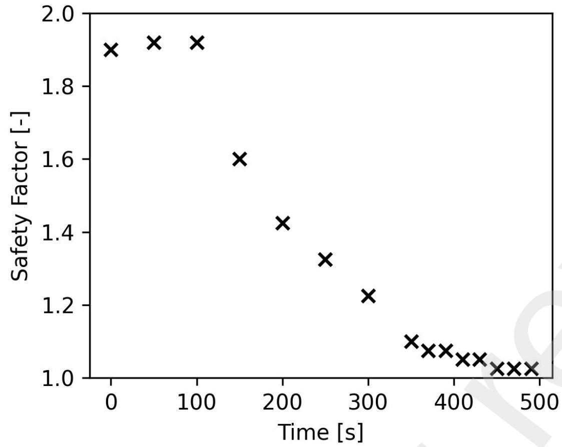

Figure 13: Safety factor evolution of the downstream slope during overtopping.

Initially, the safety factor is high, with a 1.9 value. Then, the safety factor evolves as a consequence of the changing water content, leading to a higher density but also to important cohesion losses. Finally, after 440 seconds the safety factor drops to 1.02 meaning that the dike is close to instability. The obtained failure surface is evaluated and represented on Fig.(14). Strong similarities appear between the calculated surface and the experimental one displayed[25].

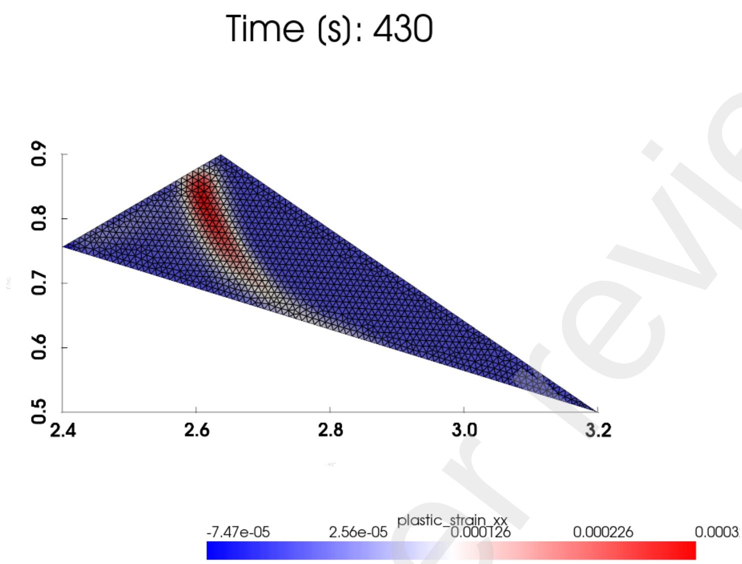

Figure 14: Failure surface: plastic strain in the x direction.

5. Conclusion

We presented an advanced model that predicts the evolution of stability in earthen embankments subjected to overtopping flows, relying solely on physical parameters. The model accounts for the impact of overtopping on the groundwater flow, which in turn influences the shear strength, the soil's density and thus the stability of the structure.

We first recalled the physical principles governing the surface-subsurface flows model, as presented in Delpierre et al. [18], which provides information on the pore pressure evolution during a given overtopping event. Secondly, we presented the constitutive law, developed by Alonso et al. [16], used to describe the relationship between pore pressure and shear strength evolution. We showed that, using this law, we were able to numerically reproduce direct shear test data, retrieved from the literature. This proves that the selection of an appropriate plastic law combined with an effective stress formulation is an adequate way of approaching the simulation of shear failure occurring in unsaturated soils.

The third part, which consists in combining the surface-subsurface flows with an appropriate effective stress formulation, is the main novelty of this work.

From the soil water retention curve and the saturated shear strength, we are able to predict the evolution of the stability of the embankment subjected to different events. We showed several theoretical applications where the model proved to perform physically. We then showed that the model is effectively able to predict the onset of failure by successfully comparing with a complex experimental failure. We were able to reproduce not only the groundwater flow, but also the failure mechanism and the onset time. With these developments we want to show that pore pressures variations effects on dams stability during overtopping events should not be overlooked.

References

[1] Tran D. K., Ralaizafisoloarivony N., Charlier R., et al. Studying the effect of desiccation cracking on the evaporation process of a Luvisol – From a small-scale experimental and numerical approach *Soil Tillage Res.*. 2019;193:142–152.

[2] Salas Jose D., Obeysekera Jayantha. Revisiting the Concepts of Return Period and Risk for Nonstationary Hydrologic Extreme Events *J. Hydrol. Eng.*. 2014;19:554–568.

[3] Foster Mark, Fell Robin, Spannagle Matt. The statistics of embankment dam failures and accidents *Can. Geotech. J.*. 2011.

[4] Tingsanchali Tawatchai, Chinnarasri Chaiyuth. Numerical modelling of dam failure due to flow overtopping *Hydrol. Sci. J.*. 2001.

[5] Pontillo Marianeve, Schmocker Lukas, Greco Massimo, Willi . 1D numerical evaluation of dike erosion due to overtopping *Journal of Hydraulic Research.* 2010.

[6] Cantero-Chinchilla Francisco Nicolás, Castro-Orgaz Oscar, Dey Subhasish. Prediction of Overtopping Dike Failure: Sediment Transport and Dynamic Granular Bed Deformation Model *J. Hydraul. Eng.*. 2019;145:04019021.

[7] Martínez-Aranda Sergio, Fernández-Pato Javier, García-Navarro Pilar. Non-Equilibrium Bedload Transport Model Applied to Erosive Overtopping Dambreach *Water.* 2023;15:3094.

[8] Van Emelen Sylvie, Zech Yves, Soares-Frazão Sandra. Impact of sediment transport formulations on breaching modelling *Journal of Hydraulic Research.* 2014:60–72.

[9] Zhu Y.. *Breach growth in clay-dikes.* PhD thesisTUDelft 2006.

[10] Swartenbroekx C., Soares-Frazão S., Staquet R., Zech Y.. Two-dimensional operator for bank failures induced by water-level rise in dam-break flows *Journal of Hydraulic Research.* 2010.

[11] Zhong Qi-ming, Chen Sheng-shui, Deng Zhao. Numerical model for homogeneous cohesive dam breaching due to overtopping failure *J. Mt. Sci..* 2017;14:571–580.

[12] Xue Ruiying, Zhang Xinhua, Cai Yujie, et al. Numerical simulation of landslide dam overtopping failure considering headward erosion *J. Hydrol..* 2021;601:126608.

[13] Bogaard Thom A., Greco Roberto. Landslide hydrology: from hydrology to pore pressure *WIREs Water.* 2016;3:439–459.

[14] Bishop A. W.. The Use of Pore-Pressure Coefficients in Practice *Géotechnique.* 1954.

[15] Alonso E. E., Gens A., Josa A.. A constitutive model for partially saturated soils *Géotechnique.* 1990.

[16] Alonso E. E., Pereira J.-M., Vaunat J., Olivella S.. A microstructurally based effective stress for unsaturated soils *Géotechnique.* 2010.

[17] Khalili N., Romero Morales Enrique Edgar, Marinho Fernando Antonio. State of the Art Report. Advances in unsaturated soil mechanics: constitutive modelling, experimental investigation, and field instrumentation 2022:297–348.

[18] Delpierre Nathan, Rattez Hadrien, Soares-Frazao Sandra. Finite-volume coupled surface-subsurface flow modelling in earth dikes *Journal of Hydraulic Research.* 2023:754–763.

[19] Soares-Frazão S. Soares, Zech Y.. Dam Break in Channels with 90° Bend *J. Hydraul. Eng..* 2002;128:956–968.

[20] Khalili N., Geiser F., Blight G. E.. Effective Stress in Unsaturated Soils: Review with New Evidence *Int. J. Geomech..* 2004;4:115–126.

[21] Lindsay Alexander D., Gaston Derek R., Permann Cody J., et al. 2.0 - MOOSE: Enabling massively parallel multiphysics simulation *SoftwareX.* 2022;20:101202.

[22] Vanapalli S. K., Fredlund D. G., Pufahl D. E., Clifton A. W.. Model for the prediction of shear strength with respect to soil suction *Can. Geotech. J..* 1996.

[23] Gan J. K. M., Fredlund D. G., Rahardjo H.. Determination of the shear strength parameters of an unsaturated soil using the direct shear test *Can. Geotech. J..* 1988.

[24] Matsui Tamotsu, San Ka-Ching. Finite Element Slope Stability Analysis by Shear Strength Reduction Technique *Soils and Foundations.* 1992;32:59–70.

[25] Awal Ripendra, Nakagawa Hajime, Kawaike Kenji, Baba Yasuyuki, Zhang Hao. An integrated approach to predict outflow Hydrograph due to landslide dam failure by overtopping and sliding *Annual Journal of Hydraulic Engineering.* 2008;52:151–156.